JOURNAL OF GEOPHYSICAL RESEARCH, VOL. 97, NO. C6, PAGES 9493-9505, JUNE 15, 1992

BRAZIL-MALVINAS CONFLUENCE: WATER MASS COMPOSITION

Keitapu Maamaatuaiahutapu,[1] Véronique C. Garçon,[1] Christine Provost,[2]
Mostefa Boulahdid,[3] and Ana Paula Osiroff[4]

Abstract. A quantitative analysis of water masses in the Brazil-Malvinas Confluence zone is performed with a least squares multiple tracer analysis using data from the confluence winter 1989 cruise. The purpose is to find the mixture of source water types that best describes the composition of a given water sample. This method is valuable in regions involving strong mixing among various source water types, as is the Brazil-Malvinas Confluence zone. Seven main core layers are identified in this region, and all are retained for the analysis : the Thermocline Water (TW), the Subantarctic Surface Water (SASW), the Antarctic Intermediate Water (AAIW), the Upper Circumpolar Deep Water (UCDW), the North Atlantic Deep Water (NADW), the Lower Circumpolar Deep Water (LCDW), and the Weddell Sea Deep Water (WSDW). Tracers selected are temperature, salinity, dissolved nutrients, and oxygen. The results show the proportion of each source water type along four east-west sections (35.4°S, 36.5°S, 37.9°S, 39°S). They are accurate to within 20% for all sources. The solution presents evidence of local recirculation of AAIW largely influenced by the two strong currents, Brazil and Malvinas. Southward TW and NADW separate from the coast, NADW turning eastward at a higher latitude than TW.

1. INTRODUCTION

The South Atlantic Ocean plays a crucial role in the global climate system due to active exchanges with neighboring oceans and local water mass modifications. To gain a better understanding and a more accurate description of the circulation of water masses, several international programs have been and are currently being carried out to investigate the dynamics of the South Atlantic Ocean. Among them, the pre-WOCE (World Ocean Circulation Experiment) Confluence program was designed to study the western boundary of the Argentine Basin.

This region is known as the Brazil-Malvinas Confluence. Two major currents, Brazil and Malvinas, meet in this zone, generating a complex array of eddies, rings, and filaments in the upper layer [Legeckis and Gordon, 1982; Roden, 1989]. Strong contrasting water types converge along the continental margin, involving complex structures within the whole water column. The large-scale aspects of the circulation and thermohaline structure have been described by Reid et al. [1977], Gordon [1981, 1989], Gordon and Greengrove [1986], Peterson and Whitworth [1989], and Reid [1989].

The Confluence program is a joint Argentine, French, and U.S. effort to provide a high-resolution picture of the dynamics of the Confluence region [Confluence Group, 1990]. Three oceanographic cruises were completed in three different seasons: austral spring, winter, and summer. Three of the various objectives of the program are (1) to obtain detailed water mass descriptions during the three seasons, (2) to detect changes in water mass composition, and (3) to study mixing and water mass transformation in winter in the area of the confluence of the Brazil and Malvinas currents.

As a first step in this direction, we performed a least squares multiple tracer analysis of water mass composition in the confluence region using Confluence 2 data, which were obtained during the winter cruise. The results confirm the present knowledge of the major water mass circulation in the western boundary of the South Atlantic Ocean and show evidence of an Antarctic Intermediate Water (AAIW) local recirculation cell and of North Atlantic Deep Water (NADW) separation from the coast.

2. METHOD

Water mass mixing and circulation patterns within the ocean are generally deduced from tracer analysis.

In principle, for deciphering the mixing of n water masses, n-1 conservative tracers are needed. Usually,

[1]Unité Mixte de Recherche 39, Groupe de Recherche de Géodésie Spatiale, Toulouse, France.

[2]Laboratoire d'Océanographie Dynamique et de Climatologie, Université Pierre et Marie Curie, Paris.

[3]Institut des Sciences de la Mer et de l'Aménagement du Littoral, Algiers.

[4]Departamento de Oceanografía, Servicio de Hidrografía Naval, Buenos Aires.

Paper number 92JC00484.
0148-0227/92/92JC-00484$05.00

the two conservative tracers, temperature and salinity, through T-S diagrams, are used to identify and track water masses. With T and S alone, only two or three source water types at the most can be considered in a quantitative water mass analysis. If more primary sources are possible, the problem is underdetermined. By including the additional constraint that mixing is dominantly isopycnal in the ocean, some sources or source water types can be ruled out as locally unavailable. However, this assumption is unrealistic in frontal regions and in areas of strong turbulent mixing.

To overcome this limitation, geochemical tracers that vary somewhat independently of temperature and salinity can be included in the water mass proportion calculations. Although nonconservative, dissolved nutrients and oxygen are used to perform multiparameter analyses of water mass composition. The principle is based on an inverse method that uses measurements of the concentration of several tracer variables to find the mixture of source water types that best describes the composition of any given water sample [Mackas et al., 1987].

Tomczak [1981] estimated the importance of cross-isopycnal mixing by computing mixing rate this way. He developed a matrix formulation in which measurements of n-1 tracers are used to solve the fractional contributions of n sources. This technique was first modified by Thompson and Edwards [1981] and later by Mackas et al. [1987]. Thompson and Edwards [1981] analyzed the formation of Antarctic Intermediate Water with this method. Mackas et al. [1987] developed the method to determine the extent of upwelled California Undercurrent Water onto the Vancouver Island shelf.

We follow Mackas et al. [1987] and add two physically realistic constraints: first, the assumed sources must sum up to 100% of the sample and second, any source contribution has to be nonnegative.

Let the vector x(n,1) give each end-member contribution to a water sample. We therefore search for the vector x which minimizes the weighted sum of squares of deviation between measured data and estimates of model parameters.
This can be written,

$$(Ax - b)^T W^{-1} (Ax-b)=\min \qquad (1)$$

with

$$\Sigma_i x_i=1$$

and

$$x_i \geq 0 \text{ for all } i$$

A is a (p+1,n) source matrix containing p tracer values for n source water types. The (p+1)th row is (1, 1,...,1) to set the first constraint.

The vector b(p+1,1) includes in its first p rows the measured values of tracer variables in a water sample. The (p+1)th row set to 1 supplies the first constraint.

W is a (p+1,p+1) dispersion matrix. It is a variance-covariance matrix tabulating the observed statistical variability in the samples and in the source water types. The weighting matrix W^{-1} is necessary because of the differences in measurement precision of the tracer variables. Temperature and salinity measurements are done with greater relative accuracy and precision than geochemical tracer measurements. So the strongest weights are put on variables measured with the best relative accuracy [Menke, 1989]. Two components of variability contribute to W: the measurement uncertainty associated with each sample and the possible error in the characterization of source water types. In practice, it is only important that the estimate of W provides an approximately correct weighting of the tracers relative to each other [Mackas et al., 1987].

The nonnegative least squares solution for x is found using the iterative algorithm described by Mackas et al. [1987]. First, the matrix W^{-1} is factored by singular value decomposition. The factors are used to transform the source definition matrix A (to a new matrix G) and the data vector b (to a new vector d) so that the problem becomes

$$(Gx - d)^T (Gx - d)=\min \qquad (2)$$

Then an iterative process permits solving (2) for x while enforcing the condition of nonnegativity [see Mackas et al., 1987].

Stability of the ouput vector x is tested by numerical perturbation experiments. They consist of adding random deviations to the measured data vector b and to the elements of the matrix A. Absolute values of the imposed deviations are lower than or equal to the estimated standard deviation values of the considered tracer variables. We can deduce a mean solution vector x for each sample. The mean solution is then compared to the nominal solution (which is computed directly from data without any perturbation) to estimate solution robustness. A variance-covariance matrix of the source composition vector x over the whole region is also estimated.

The tracer error vector (Ax-b) is the difference between the predicted (Ax) and the measured (b) data. This vector provides information about nonconservative behavior of tracers and possible errors made on source water types description and on data measurements. Thus in an ideal case

(where source water type descriptions are correct and complete, measurements unbiased, and tracers conservative), the vector (Ax-b) should be null. A relative goodness of fit can be determined with the weighted mean square tracer error (residual) which is written,

$$D^2/(p+1)=(p+1)^{-1}\ (Ax-b)^T\ W^{-1}\ (Ax-b)$$

If W has adequately normalized the residual tracer variability, the residuals should be distributed as χ^2/ν. The number of degrees of freedom ν is approximately $p-n_f+1$, and n_f is the number of source types retained in the final solution.

3. WATER MASSES

3.1. Data

The Confluence 2 data were collected aboard the R/V *Oca Balda* during the austral winter of 1989 (September 3-13). The 28 conductivity-temperature-depth (CTD) casts performed during the Confluence 2 cruise were distributed along four east-west sections across the continental slope (Figure 1).

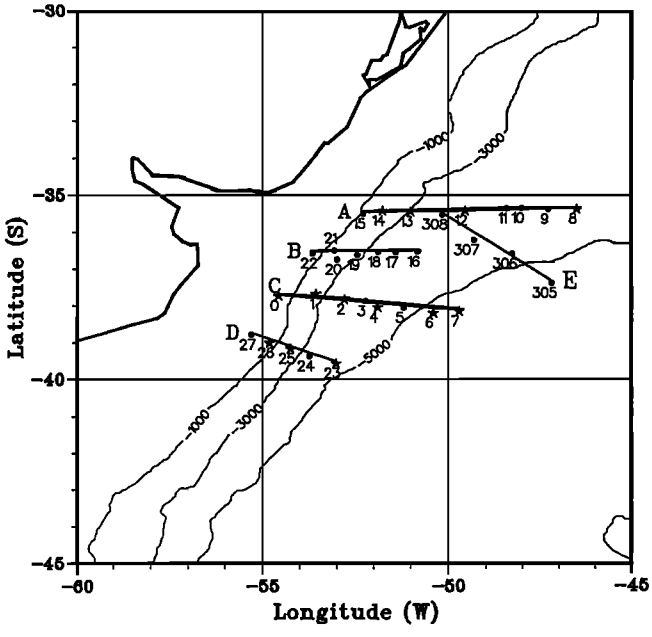

Fig. 1

Fig. 1. Location of CTD stations of the oceanographic cruises Confluence 2 (sections A, B, C, D; September 1989) and SAVE (leg 5; section E, March 1989). The 1000-, 3000-, and 5000- m isobaths are shown. The stars represent the Confluence 2 CTD stations with TCO_2 vertical profile.

Seawater samples were collected from a 12-Niskin-bottle CTD rosette. All casts went close to the bottom. A surface cast of up to four bottles was added to the unique cast in order to increase the vertical resolution in the upper ocean. Tracer analysis tasks were shared among the different participants of the Confluence program.

The CTD analysis and dissolved oxygen concentration measurements were carried out by the Oceanography Department of the Hydrographic Service of Argentina.

Measurements of the CO_2 partial pressure and total CO_2 in seawater were accomplished by T. Takahashi's group from the Lamont-Doherty Geological Observatory of Columbia University [Takahashi et al.,1990].

Nutrient concentrations (silica, phosphate, nitrate and nitrite) were measured by the French scientists of Unité Mixte de Recherche (UMR) 39 and Laboratoire d'Océanographie Dynamique et de Climatologie (LODYC) in collaboration with the Algerian Institut des Sciences de la Mer et de l'Aménagement du Littoral (ISMAL). The automated analyses for nutrient determination were performed either immediately after sampling or after a few hours storage in a 4°C cold room. They were made using a Technicon Autoanalyzer AAII according to the techniques described by Boulahdid [1987]. The instantaneous analytical reproducibility was established on deepwater replicate samples at CTD stations 7 and 22. In the worst cases nitrate, phosphate, and silicate measurements (expressed in the coefficient of variation) are obtained with a reproducibility of 0.5%, 0.8% and 0.9%, respectively. A comparison was carried out between Confluence 2, Geochemical Ocean Sections Study (GEOSECS), and South Atlantic Ventilation Experiment (SAVE) leg 5 data on deep waters to detect the presence of systematic errors. When necessary, the appropriate corrections were applied to the Confluence 2 data [Garçon et al.,1991].

3.2. Zonal Sections

Confluence 2 section C at 38°S (Figure 2) is chosen to illustrate the characteristics of the various source water types moving around the confluence region. Original data of the three sections A, B, and D are presented by Charo et al. [1991] and A.R. Piola et al. (unpublished manuscript, 1992).

Earlier studies [Reid et al., 1977; Gordon, 1981; Gordon and Molinelli, 1982; Peterson and Whitworth, 1989; Reid , 1989] globally distinguish seven core layers within the whole water column in the southwestern Atlantic around the confluence region. All tracer extrema

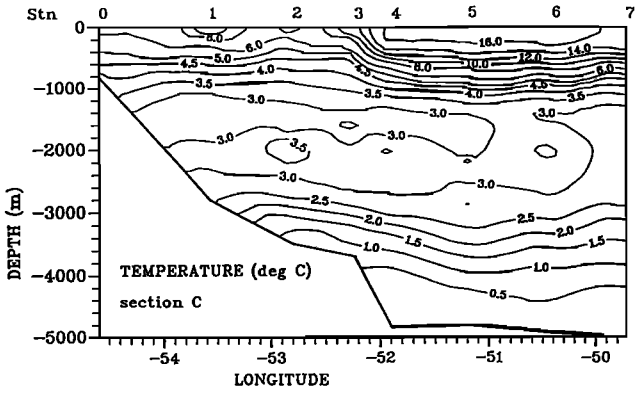

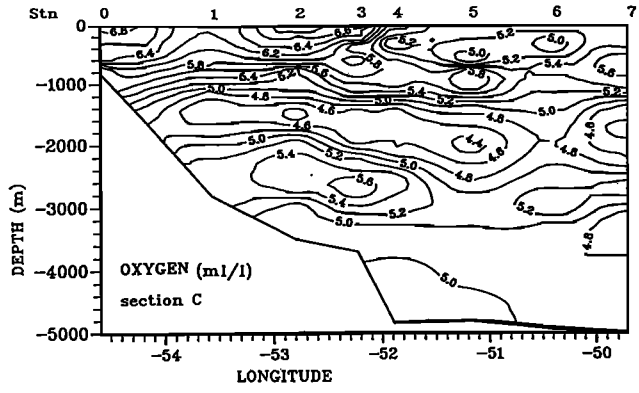

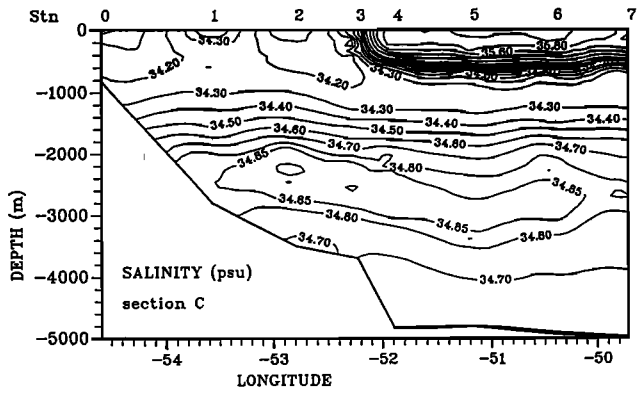

Fig. 2a

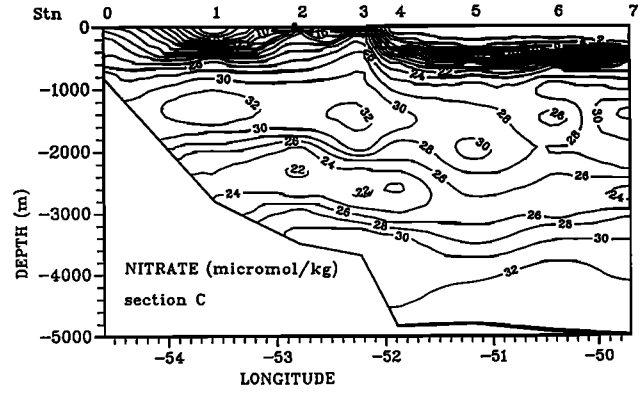

Fig. 2b

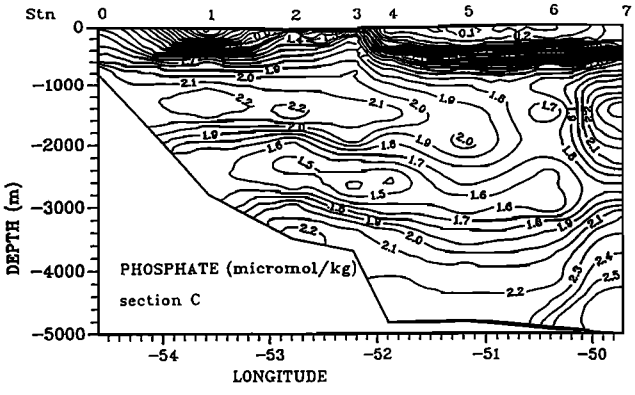

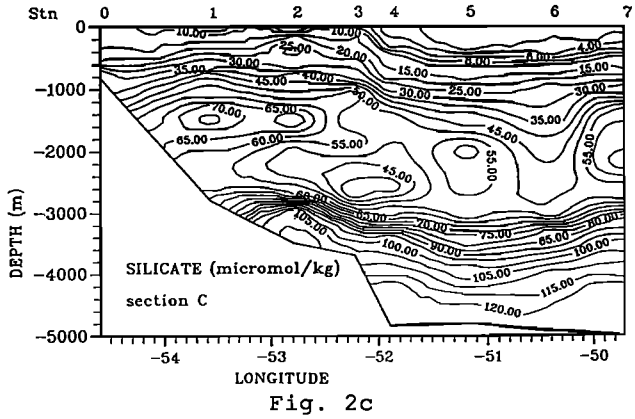

Fig. 2c

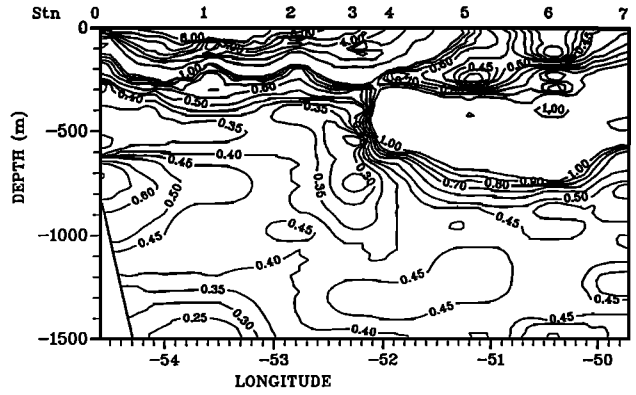

Fig. 2d

Fig. 2. (a) In situ temperature (°C) and salinity (psu); (b) oxygen (ml l^{-1}) and nitrate (μmol kg^{-1}); (c) phosphate (μmol kg^{-1}) and silicate (μmol kg^{-1}); (d) potential vorticity (10^{-10} m^{-1} s^{-1}) for the upper 1500 m, along the Confluence 2 section C indicated in Figure 1.

seen on Confluence 2 section C (Figure 2) can be associated with the different core layers.

Within the upper level, the strong thermohaline gradient observed at 38°S (Figure 2) is due to the confluence of the Brazil and the Malvinas currents. Characteristics of waters brought by these two currents are sharply contrasted. Water entering the confluence area from the north with the Brazil Current is the warmest and the saltiest water, with the most intense thermocline oxygen minimum; it is called here the Thermocline Water (TW). It occurs in the eastern part of the section between stations 3 to 7. The lowest nutrient (nitrate, phosphate, silica) concentrations are also found in the eastern part of the section (stations 4 to 7). At 38°S, the TW meets the northward flow of Subantarctic Surface Water (SASW), observed in the western part of the section (stations 0 to 3). It is conveyed by the Malvinas Current, which is cooler, less saline, and richer in oxygen than the Brazil Current. A core of salinity minimum, found beneath the TW, marks the Antarctic Intermediate Water (AAIW) and extends from stations 4 to 7. This salinity minimum tongue is linked with very low salinity values in the west near the surface. Since the AAIW is advected in the confluence region by the Malvinas Current, it flows from the surface in the cyclonic loop of the Subantarctic front to reach its greatest depth (800-1000 m) [Piola and Gordon, 1989]. This salinity minimum parallels the 4°C isotherm and coincides with a local oxygen maximum. Roden [1989] shows local minimum of potential vorticity associated with the AAIW in the Argentine basin. This minimum is observed on section C from stations 0 to 3 around 500 m. At station 3, this minimum plunges to reach 1000 m depth beneath the thermocline. The oxygen minimum core discussed by Reid et al. [1977] corresponds to the Circumpolar Deep Water (CDW). The CDW flows northward as a single core south of 50°S where it separates into two branches: the upper CDW (UCDW), above the North Atlantic Deep Water (NADW), and the lower CDW (LCDW), below the NADW. On Confluence 2 section C (Figure 2), between 1200 m and 2000 m, the cold (<3°C), minimum oxygen core layer extends from west to east with a contraction of the oxygen isolines at station 6. It is associated with a relative maximum in phosphate, nitrate, and silica in the western part of the section. The main core of the North Atlantic Deep Water is distinguished between 2000-2500 m by high values in salinity and temperature (stations 1 to 6). At the same depth level, higher oxygen and lower nutrient concentrations than in neighboring waters are observed between stations 2 and 5. This salinity maximum is slightly below the depth of the temperature maximum. The second oxygen minimum corresponding to the LCDW is only a small limb on the east of section C (Figure 2). The abyssal layer, the Weddell Sea Deep Water (WSDW), generally considered as the coldest water with temperature lower than 0° C [Georgi, 1981a], spreads northward. This water, observed between stations 4 and 7, has relatively high content of nutrients.

4. APPLICATION OF THE METHOD

4.1. Matrices A and W

The application of the multiparameter analysis of water mass composition to Confluence 2 data requires the determination of matrices A and W.

Matrix A contains the characteristics of the source water types evolving in the Confluence region. The seven source water types mentioned above (TW, SASW, AAIW, UCDW, NADW, LCDW, WSDW) are all retained in our analysis. Tracers selected are temperature, salinity, dissolved oxygen, and nutrients. Considering the particular characteristics of the seven previous water masses, we arrive at the source characterizations (Table 1) by compiling historical data [Reid et al., 1977; Bainbridge, 1981; Gordon, 1981,1989; Georgi, 1981a, b; Gordon and Molinelli, 1982; Greengrove, 1986; Peterson and Whitworth, 1989; Roden, 1989; Piola and Gordon, 1989]. The source types TW, SASW, AAIW, UCDW, NADW, LCDW, and WSDW are typical of the σ_0 26.36, 26.96, the σ_1 31.76, 32.26, the σ_2 36.99, and the σ_4 45.92, 46.14 surfaces, respectively, and the values in matrix A are chosen in regions close to our studied area.

In this inverse computation we have to define a weighting matrix W. High weights (low values in W) are given to tracers measured with the greatest relative accuracy. Water mass variability also contributes to W. A water mass travelling from one point to another has its properties changed in the stirring and mixing processes. We evaluate these properties variations for a water mass around its proper isopycnal along its whole path throughout the studied area. Strong variations are found for upper level water masses. We then choose to adjust our tracer variances on deep source water type tracer deviations. These numbers are underestimated for surface waters subject to stronger variability. For simplicity, we take a diagonal weighting matrix W, thereby assuming no covariance between tracers (Table 1). This is a strong hypothesis; in reality, oxygen concentration depends on temperature and concentrations of the various nutrients are related (e.g., Redfield ratios). However, the ratio of

Table 1. Tracer Characteristics of Primary Source Water Types Compiled From Historical Data and Estimated Standard Deviation For Each Tracer

Tracers	MATRIX A							
	TW (x1)	SASW (x2)	AAIW (x3)	UCDW (x4)	NADW (x5)	LCDW (x6)	WSDW (x7)	MATRIX W: σ
T, °C	16.0	5.0	4.0	2.5	3.00	1.50	-0.20	0.25
S, psu	35.8	34.1	34.2	34.6	34.92	34.76	34.68	0.07
NO_3^-, µm/kg	6.0	17.0	26.5	29.0	23.50	29.00	31.00	1.12
PO_4^{3-}, µm/kg	0.5	1.9	1.9	2.2	1.70	1.80	2.20	0.15
SiO_2, µm/kg	5.0	10.0	20.0	70.0	30.00	102.00	121.00	1.50
O_2, ml/l	5.4	6.0	5.6	4.6	5.60	4.75	5.25	0.13
$\Sigma_i x_i=1$	1.0	1.0	1.0	1.0	1.00	1.00	1.00	0.01

The weighting matrix is derived by inverting the matrix $W = \sigma^2 I$, where I is the identity matrix.

the largest to the smallest eigenvalues for the whole matrix G (equation (2)) is 3000. This value obtained when the nonnegativity constraint is not taken into account shows that the variables are quite independent. When the nonnegativity constraint is considered (next step in the iterative process), the rank of the system diminishes and the conditioning of the reduced matrix is improved.

4.2. Robustness of the Results

The inversion performed with the six tracers mentioned above leads to the results presented in Plates 1-4. They show the concentration of each source water type along the four sections. These results correspond to the mean solutions obtained after perturbation. One hundred perturbations are performed on each sample. The comparison with the nominal solution (not shown here) reveals no great differences between the mean solution and the nominal solution. The sensitivity of each source water type in each sample can be expressed by a standard deviation value. In the worst case, values of 2%, 9%, 18%, 15%, 21%, 19%, and 11% are found for the sources TW, SASW, AAIW, UCDW, NADW, LCDW, and WSDW, respectively. The solution displayed in Plates 1-4 can therefore be assumed accurate to within about 20% for all sources. The dispersion matrix over the region of the output vector x is reported in Table 2. The standard deviation of each element of x is given by the square root of the corresponding diagonal element in this matrix. The greatest deviation is obtained for TW. The TW properties variation over a wide range (temperature and salinity mainly) may be at the origin of this high value.

4.3. Residuals

The elements of the tracer error vector (Ax-b) present high absolute values at some locations. The criterion of goodness of the fit to the model is defined in terms of χ^2 for each sample. Residuals ($D^2/(p+1)$) are distributed as χ^2/ν. Samples which have residuals larger than 1.4 are considered as showing poor fit.

We find that most samples with poor fit are near the sea surface (Figure 3). Two reasons may be put forward: the local nonconservativeness of tracers and the poor characterization of water masses. Indeed, biological activity, intense in the euphotic zone, acts as a sink for nutrients and as a source for dissolved O_2. Gas exchange at the air-sea interface controls the O_2 evolution. We therefore overestimate nutrients and underestimate O_2 in the upper ocean in our description. The surface waters also have their T-S properties affected by direct warming or cooling from the atmosphere. The T-S properties largely vary in regions where double diffusion process occurs such as at the TW-AAIW interface [Gordon, 1981]. The water samples are not always perfectly represented by the water masses described in Table 1. Other source water types surely contribute to the melting pot. Our SASW component is in fact a mixture of slope water, river plume water from Río de la Plata, and real SASW advected by the Malvinas Current [see Gordon, 1981]. It is difficult to give tracer characteristics to TW and SASW waters because tracers have such a broad range of variation (e.g., for TW, temperature can vary from 10°C to 18°C). Here, the TW includes the warmest and/or

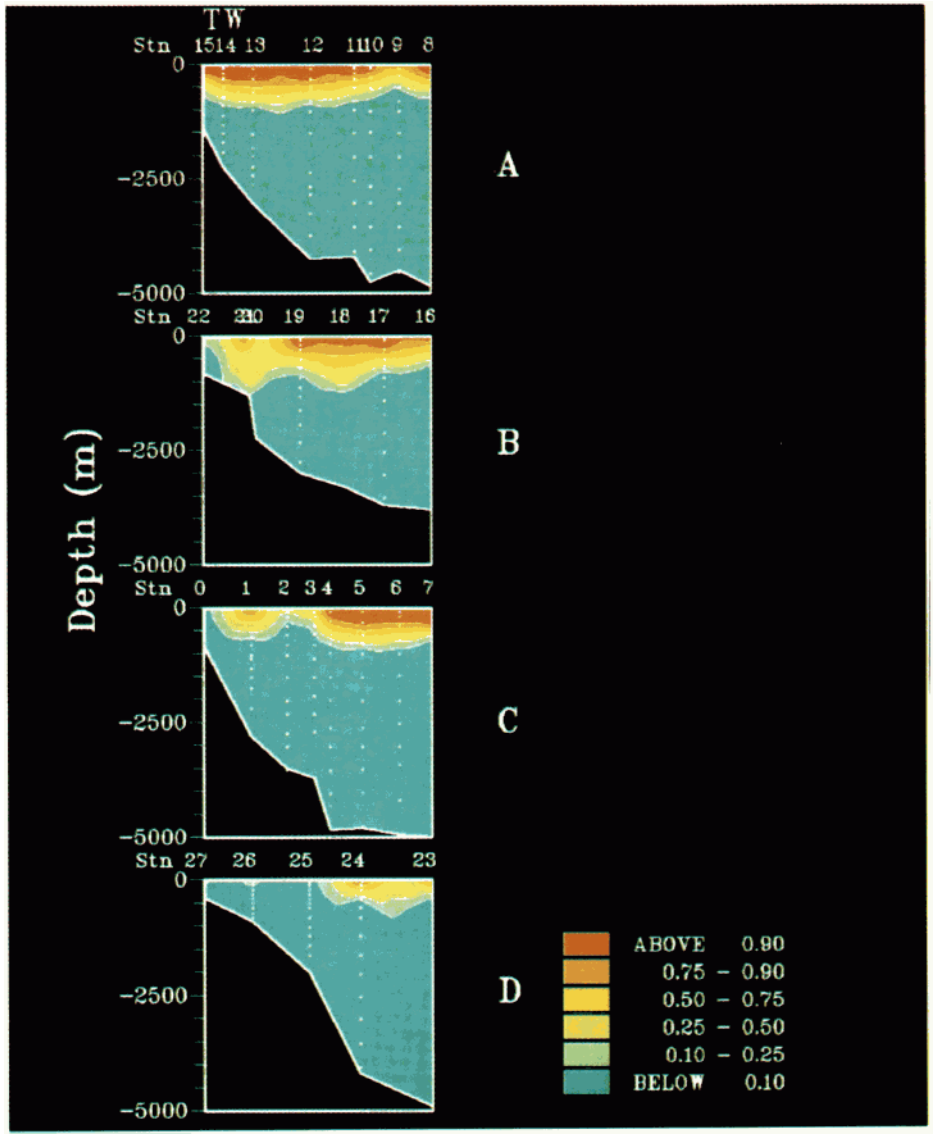

Plate 1. Source composition solution showing concentration (0 to 1.0, or 0 to 100%) of TW for the four Confluence 2 sections: (a) A, (b) B, (c) C, and (d) D. Sample locations are indicated by dots. Contours and shading indicate the estimated 0.1, 0.25, 0.50, 0.75 and, 0.90 source concentration isopleths.

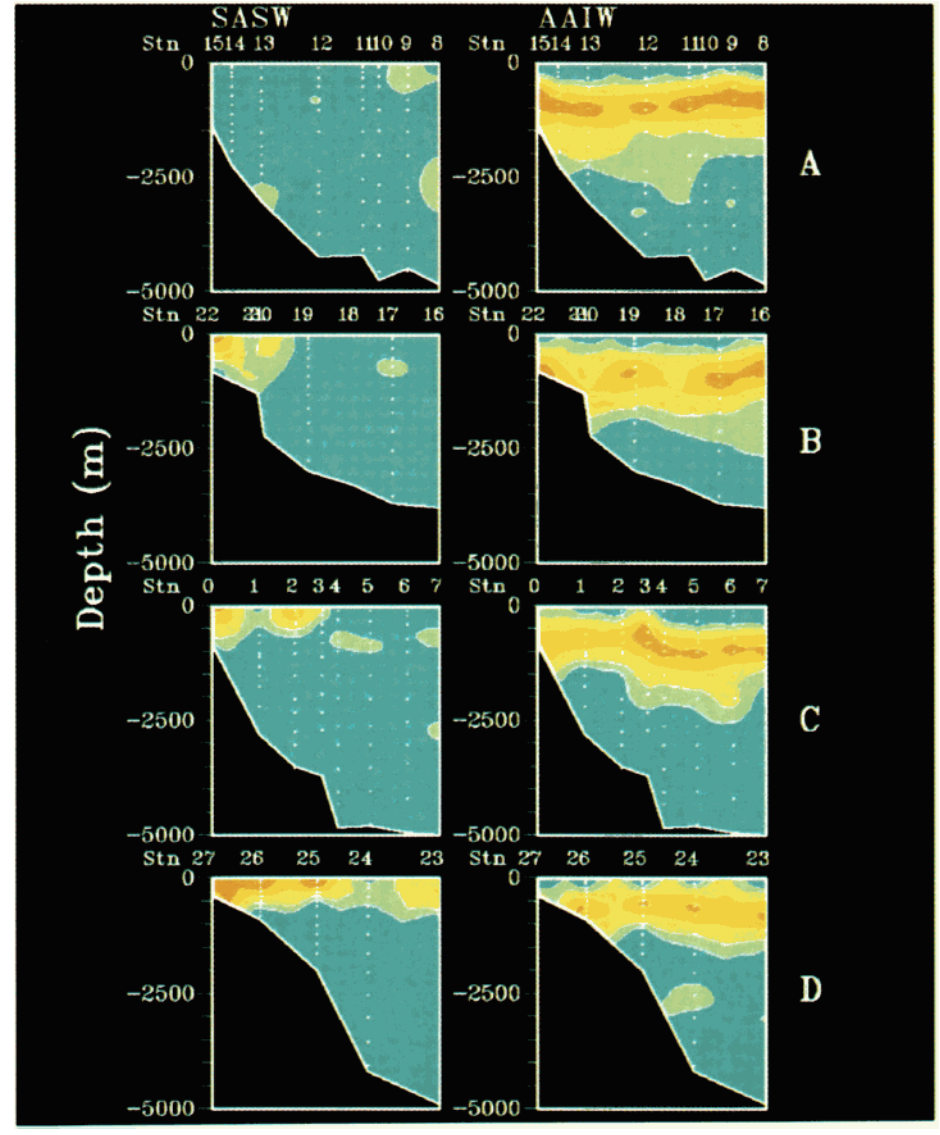

Plate 2. Source composition solution showing concentration of SASW and AAIW for the four Confluence 2 sections: (a) A, (b) B, (c) C, and (d) D. Sample locations are indicated by dots. Contours and shading indicate the estimated 0.1, 0.25, 0.50, 0.75, and 0.90 source concentration isopleths (see Plate 1 for color scale).

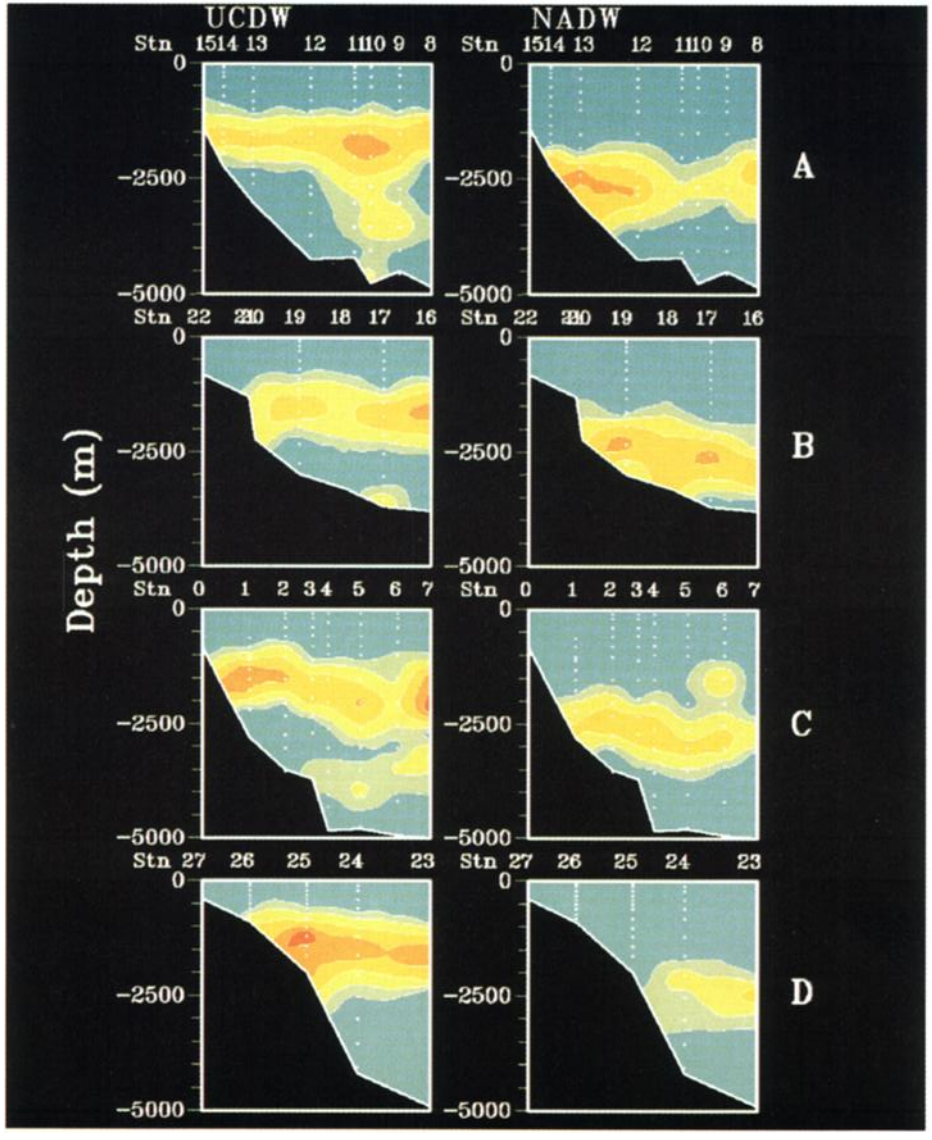

Plate 3. Source composition solution showing concentration of UCDW and NADW for the four Confluence 2 sections: (a) A, (b) B, (c) C, and (d) D. Sample locations are indicated by dots. Contours and shading indicate the estimated 0.1, 0.25, 0.50, 0.75, and 0.90 source concentration isopleths (see Plate 1 for color scale).

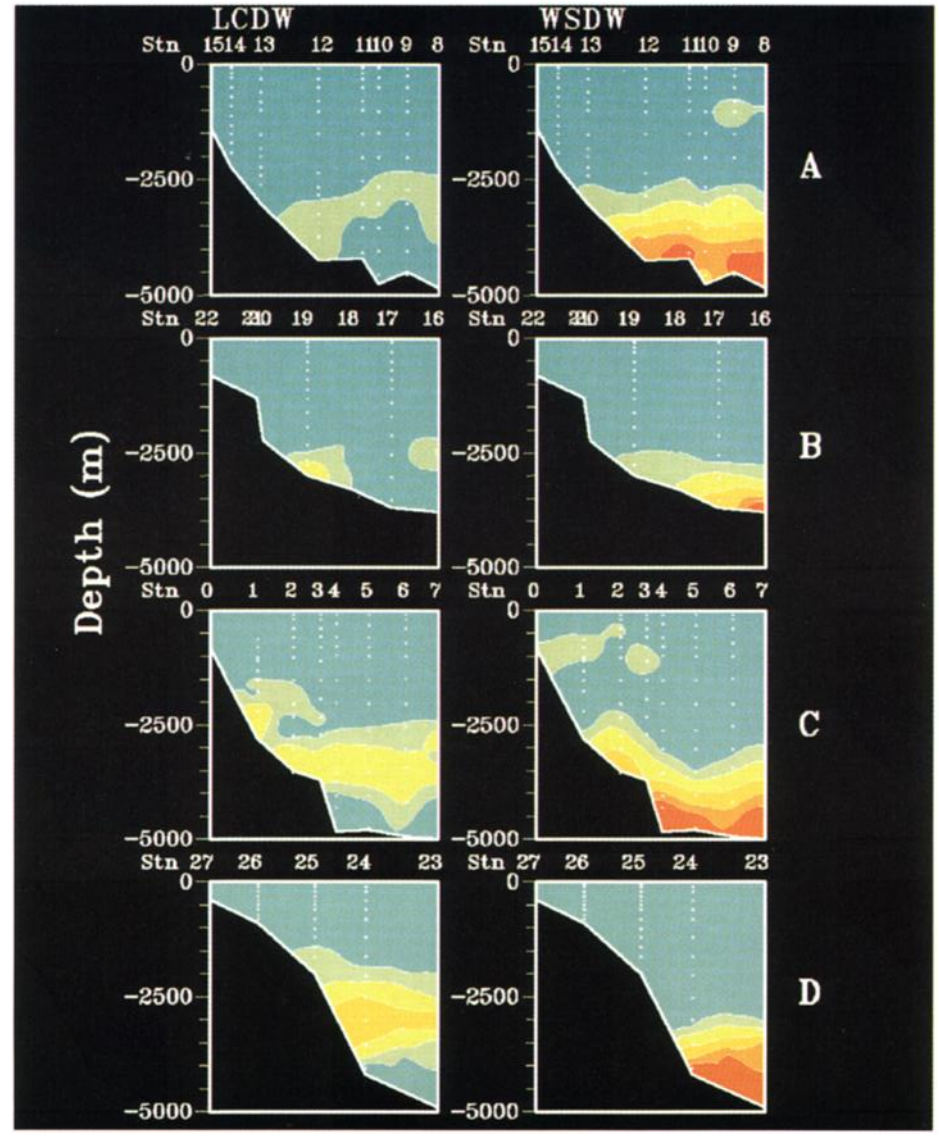

Plate 4. Source composition solution showing concentration of LCDW and WSDW for the four Confluence 2 sections: (a) A, (b) B, (c) C, and (d) D. Sample locations are indicated by dots. Contours and shading indicate the estimated 0.1, 0.25, 0.50, 0.75, and 0.90 source concentration isopleths (see Plate 1 for color scale).

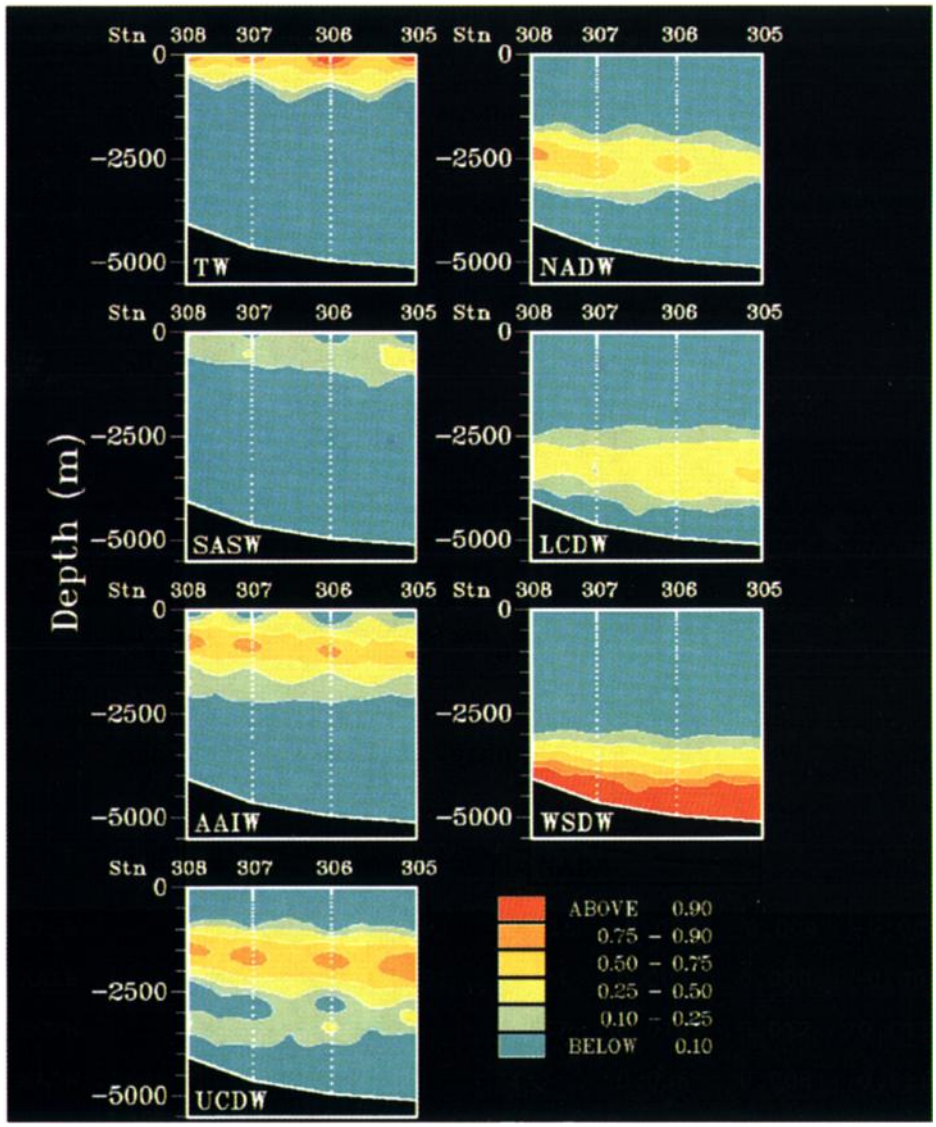

Plate 5. Source composition solution showing concentration (0 to 1.0) of the seven source water types versus horizontal position and depth for the SAVE - leg 5 section.

Table 2. Estimated variance and covariance of elements of the source composition solution vector x

	TW	SASW	AAIW	UCDW	NADW	LCDW	WSDW
TW	0.170	-0.017	0.013	-0.021	-0.016	-0.008	-0.019
SASW		0.075	0.003	-0.015	-0.008	-0.004	-0.006
AAIW			0.091	0.024	0.003	0.000	-0.003
UCDW				0.067	0.016	0.012	0.011
NADW					0.036	0.008	0.016
LCDW						0.010	0.011
WSDW							0.046

saltiest waters; the SASW contains all the waters with low salinity and warmer than AAIW.

Evidence of local nonconservativeness of tracers around 1500 m is observed (Figure 3). This is mainly due to oxygen consumption and nutrient release.

Similarly, scattered dots within bottom waters (4000-5000 m) are essentially the result of poor prediction for silicate values.

5. RESULTS AND DISCUSSION

5.1. The Upper Layer

5.1.1. The Thermocline Water. The TW is carried into the confluence area by the southward Brazil Current. The TW has high concentrations on section A (35.4°S) near the surface (Plate 1). It contributes to water samples for more than 93% from station 10 to 15 where it forms an homogeneous thick layer (average thickness of 240 m). The thermocline depth varies from the coastline to the east. On the shelf break, at station 15 (96% at 200 m) it is deeper than at station 10 (98% at 100 m). At station 9 the isolines rise (>60% at 100 m). The TW progresses southward and separates from the continental shelf. At 36.5°S (section B) the TW leaves the shelf break (9% at station 22 at 100 m). It is still well concentrated at stations 19 and 17 (> 84% at 300 m). The thermocline depth decreases at station 16 (100% at 81 m and 54% at 300 m). On section C (37.9°S), the TW completely leaves the shelf (30% at 100 m at station 3). Highest concentrations are between stations 4 and 7 (> 96% until 350 m at station 5). On the southern section D (39°S), the TW contributes to 90% to the water sample only at station 24 (53.7°W) and near the surface.

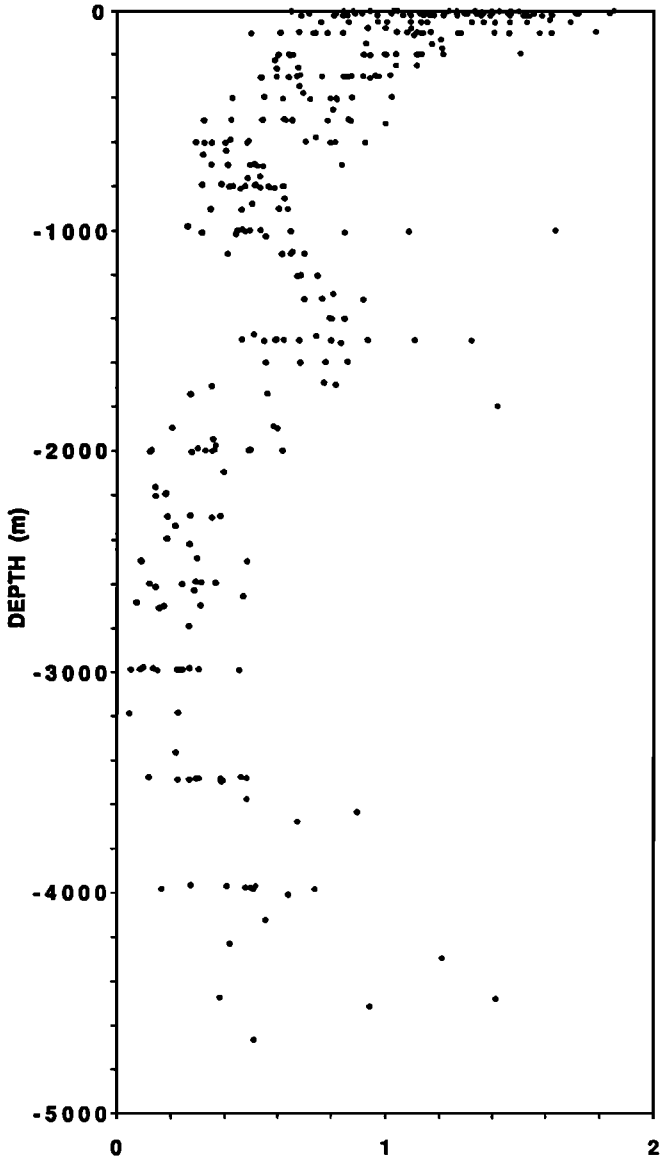

Fig. 3. Residuals (equal to $(Ax-b)^T W^{-1} (Ax-b)/(p+1)$) versus depth for all Confluence 2 stations.

The TW leaves the coast and its western boundary (considered here as the limit where the contribution falls below 90%) evolves to the east from 52.44°W at 36.6°S to 52.2°W at 37.8°S. This boundary is eroded and warm cores separate from the homogeneous TW layer (stations 1 and 20). Winter deep convection favored by the Brazil Current extension [Gordon, 1981] contributes also to the rapid erosion of the TW.

The TW patterns (Plate 1) fit in with the temperature patterns (Figure 2 and Charo et al. [1991]). On all sections, the high concentration of TW is included in the area delimited by the strong thermocline. The western boundary of the southward Brazil Current carrying the TW into the confluence area coincides with that of the surface water thermal front.

The TW is marked by a deep and strong thermocline until it reaches the latitude 37.9°S and a thin portion of TW is observed at 39°S. The deep TW limit varies also zonally at stations 9 and 2, where TW becomes much shallower. This strong depth variation is due to intrusions of waters with very different characteristics.

5.1.2. The Subantarctic Surface Water. Highest contributions (Plate 2) are found in the south and close to the shelf break (contribution higher than 90% at stations 25, 26, 27, 0, and 22). A homogeneous layer, 200 m thick, is observed between stations 25 and 27 with a contribution over 90%. The concentrations of SASW decrease simultaneously northward, eastward, and with depth. The upper eastern limit of SASW (visualized on sections B, C, D) follows a curved line from station 25 (54.25°W) to station 22 (53.7°W) going through station 0 (54.3°W). On section B, SASW is compressed along the western boundary above the continental shelf. At 35°S, this source type is nonexistent in the

water sample (e.g. contribution lower than 10% at station 15).

Little SASW is encountered in our results. Two explanations can be given. First, at those latitudes the Malvinas Current which conveyed the SASW is surely compressed onto the continental shelf by the southward extension of the Brazil Current. The CTD stations might not be located far enough in the west. Second, the signal of SASW in our description corresponds to the northern limb of SASW [Legeckis and Gordon, 1982].

5.2. The Antarctic Intermediate Water

In the confluence region, the intermediate core layer (AAIW) extends within the depth range of 500-1100 m (contribution higher than 60%) (Plate 2). On section A, AAIW has a well identified core underlying the TW between stations 10 and 14, with a contribution larger than 75% within the depth range of 800-1100 m. The isoline of 80% concentration of AAIW is found at shallower depth (500-800 m) at stations 9 and 15. On section B, AAIW contributes to more than 80% between 600 m and 1100 m. On section C, one always observes a high contribution of AAIW, up to 80% around 1000 m from stations 4 to 7. In the west (stations 0 to 3), the same fraction values are found between 600 m and 800 m. At station 3, 90% of AAIW fraction is obtained around 500 m. On the southernmost section, concentrations higher than 80% are observed at stations 23 and 24 at the average depth of 700 m, at station 25 at shallower depth (450 m) and in the west (station 26) around 600 m.

Advected in the confluence region by the Malvinas Current [see Piola and Gordon, 1989], the AAIW is found at shallower depth within the Malvinas Current, where it forms a blend with SASW. Similarities between AAIW and SASW have been showed by Gordon [1981]. When the cold SASW meets the TW, it spreads beneath the thermocline [Gordon, 1981] and forms the AAIW found at a greater depth.

The most intriguing result is that the AAIW concentration decreases from the northernmost section to the southernmost section. The subthermocline AAIW forms a homogeneous concentrated core. The AAIW, characterized by its low salinity value, is as well defined in the north as in the south under the TW (Figure 2 and Charo et al. [1991]). In regions where AAIW and SASW intermingle, there is no well-separated salinity minimum core, and salinity increases monotonically with depth.

The high concentration in the north indicates that the cold water from the south does not gently spread northward below the TW. If one considers the high northern AAIW concentration values and the spreading of AAIW advected by the Malvinas Current, unless the SASW is found onto the continental shelf at 35°S, the only explanation left is that part of the AAIW is recirculated within the anticyclonic gyre. The hypothesis that SASW only feeds the AAIW cannot be supported here, because the quantity of AAIW found underneath the TW is too considerable. One possible route of the AAIW could then be the following: AAIW is carried northward along the western boundary [Piola and Gordon, 1989]. Around 40°S, it flows around the great anticyclonic gyre eastward, northward, and westward to the boundary again [Reid, 1989]. There, the AAIW from the south recoalesces along the frontal zone with recirculated AAIW by the subtropical gyre, and the new blend accompanies the Brazil Current in its southward route.

5.3. The Deep Layers

An 80% core of UCDW extends at an average depth of 1500 m on the four sections (Plate 3). The UCDW concentration is higher on the southern sections (C, D) than on the northern ones (A, B). Its contribution decreases monotonically northward on the continental slope from 99% (station 25, 1200 m) to 60% (station 13, 1500 m). At 35.4°S, contributions above 50% are found at stations 9, 10, and 11 at a deeper level between 1500 m and 2000 m. At 37.9°S, the UCDW fraction is 46% at 2000 m. In the west (stations 1 and 2) the UCDW vein of contribution above 50% is detected between 1000 and 1700 m. The 50% band is tilted from stations 3 to 5 and returns to horizontal at a depth higher than 2000 m between stations 5 and 7.

The NADW is compressed against the continental slope on the northernmost section: higher than 83% at stations 12-13 and at about 2500 m (Plate 3). Its southward spreading is accompanied by a strong decrease in the west (concentration lower than 40% close to the continental slope on section D). The NADW moves away from the continental slope between 37.9°S and 39°S and thus higher contributions are found in the east. A parcel of NADW upwells at station 6 (60% at a depth of 1500 m).

The LCDW, like the UCDW, has the highest contributions close to the continental slope on the southernmost section (60% at 3000 m at stations 23 and 24) (Plate 4). Its concentration decreases rapidly toward the north. On section C, it is less than 50%. Further north, the LCDW is nearly nonexistent.

The WSDW is well marked (higher than 90%) on the bottom (Plate 4). On section D, WSDW is greater than 38% beyond 3500 m. At station 2, a 20% contribution is found at 2300 m. Some cells are observed at shallower depths.

This description of the deep layers is consistent with the circulation pattern

given by Reid et al. [1977]. We see (Plate 3) that the UCDW layer is separated into two branches, one moving eastward in the anticyclonic gyre as suggested by Reid et al. [1977] and the other one confined near the slope. The latter progresses northward against the continental slope and follows the Malvinas Current. Its concentration decreases rapidly between stations 1 and 19.

This temporary confinement initiates mixing between UCDW and NADW (section B). The confluence area represents the region where the CDW is submitted to the greatest change in its properties before running eastward [Georgi, 1981b].

The NADW flows southward along the western boundary and turns eastward near 40°S [Reid et al., 1977]. Our proportions pattern (Plate 3) localizes the separation from the slope at about 38°S and shows the net decrease of NADW concentration towards the south. The encounter of NADW and CDW produces small structures between the deep waters (station 6).

Although divided into two parts on the southernmost section in our description, the CDW forms one single core, extending within the depth range of 1000 m to 4000 m. Spreading north, the major contributions of CDW join the UCDW. The lower branch progressing northward is forced back by NADW and/or moves eastward with NADW. This description is in agreement with the little tongue of oxygen minimum observed in Figure 2. The LCDW eastward shift is also in part due to the strong presence of WSDW on the bottom floor.

6. CONCLUSION

The constrained least squares method (LSM) gives a useful quantitative analysis of water mass composition in the Brazil-Malvinas Confluence. This is a very complex region with respect to its water mass structure (as much as seven different water masses are present) and to its dynamics (frontal region with intense mixing activity and water mass transformation). Conventional T-S analysis, which needs the hypothesis of isopycnal mixing to discriminate between three water masses (at the most), cannot be used. The LSM well defines the limits between the different water types and provides a good description of the core layer location by gathering information brought out by the different tracers. Geochemical tracers are useful in discriminating many source water types at once in such a small region and in revealing small structures.

The low vertical sampling resolution performed during the Confluence 2 cruise could have been a problem. The comparison between the Confluence 2 (Plates 1-4) and the SAVE - leg 5 results (Plate 5) gives us some confidence that this is not the case. Indeed, the water masses seem as well identified with the Confluence data set than with SAVE even though SAVE sampling has a more refined vertical resolution (typically 36 water samples rather than 16).

An inversion with total CO_2 as an additional tracer was also performed. The sparsity of the TCO_2 data (Figure 1) precluded any good interpolation of the solution. However, whenever possible, a comparison with the results of Plates 1-4 showed that the main structures of each core layer do not change significantly. Therefore, the amount of TCO_2 data available did not bring any new information in the mixing analysis.

The results are in agreement with the present knowledge of the water masses circulation in the confluence region. The new information is the larger quantity of AAIW in the north beneath the strong thermocline than in the south from where the AAIW is derived. This shows evidence of local recirculation of AAIW by the subtropical gyre. In the deep layers, small structures found here emphasize the role played by the stirring processes as suggested by Georgi [1981b].

Ongoing analysis of the spring and summer confluence data sets will allow the detection of changes in water mass composition and mixing. It will give insight into the seasonal and interannual variability of the thermodynamical processes in the region and constitute a valuable tool for designing future sampling strategy at sea in this area.

Acknowledgments. We would like to thank Taro Takahashi for providing us Confluence 2 CO_2 data, yet unpublished at the time we performed this analysis. We are also grateful to William Smethie for allowing us to use unpublished data of the SAVE - leg 5. We acknowledge the dedicated efforts of the officers and crew of the Argentine research vessel *Oca Balda*. Comments by J.-F. Minster, A.R. Piola, J. Reid, and two anonymous reviewers are greatly appreciated. The project was funded by a grant of the Centre National de la Recherche Scientifique (PNEDC : CO_2, WOCE) to UMR39 and LODYC.

References

Bainbridge, A.E., GEOSECS Atlantic Expedition, vol. 1, Hydrographic Data 1972-73, 120 pp., U.S. Government Printing Office, Washington D.C., 1981.

Boulahdid, M., Analyse des sels nutritifs dans l'eau de mer. Etude du mélange des masses d'eau et de l'oxydation de la matière organique

dans l'océan, Thèse de Doctorat, 266 pp., Univ. Paris VII, 1987.

Charo, M., A.P. Osiroff, A. Bianchi, and A.R. Piola, Datos fisico-chimicos, CTD y XBT, Campañas oceanograficas Puerto Deseado 02-88, Confluencia 88 y Confluencia 89, Inf. Tec. 59/1991, 422 pp., Buenos Aires, Serv. de Hidrogr. Nav., 1991.

Confluence Group, Confluence 1988-1990: An intensive study of the southwestern Atlantic, EOS Trans. AGU, 71(41), 1131-1134, 1990.

Garçon, V.C., M. Boulahdid, K. Maamaatuaiahutapu, and B-Y Boudjellal, Rapport des campagnes à la mer Confluence-1, novembre 1988; Confluence-2, septembre 1989; Confluence-3, février 1990: Données de sels nutritifs, Rapp. interne UMR 39/GRGS 91.103., 207 pp., Groupe de Recherche de Géodésie Spatiale, Toulouse, 1991.

Georgi, D.T., Circulation of bottom waters in the Southwestern South Atlantic, Deep Sea Res., Part A, 28(9), 959-979, 1981a.

Georgi, D.T., On the relationship between the large-scale property variations and fine structure in the circumpolar deep water, J. Geophys. Res., 86(C7), 6556-6566, 1981b.

Gordon, A.L., South Atlantic thermocline ventilation, Deep Sea Res., 28, 1239-1264, 1981.

Gordon, A.L., Brazil-Malvinas confluence--1984, Deep Sea Res., 36, 359-384, 1989.

Gordon, A.L., and C.L. Greengrove, Geostrophic circulation of the Brazil-Falkland Confluence, Deep Sea Res., 33, 573-585, 1986.

Gordon, A.L., and E. Molinelli, Southern Ocean Atlas: Thermohaline and Chemical Distributions, 11pp., 233 illustrations, Columbia University Press, New York, 1982.

Greengrove, C.L., Thermohaline alteration of the South Atlantic pycnocline, Ph.D theais, 211 pp., Columbia Univ., New York, 1986.

Legeckis, R., and A.L. Gordon, Satellite observations of the Brazil and Falkland currents--1975 to 1976 and 1978, Deep Sea Res., 29, 375-401, 1982.

Mackas, D.L., K.L. Denman, and A.F. Bennett, Least squares multiple tracer analysis of water mass composition, J. Geophys. Res., 92(C3), 2907-2918, 1987.

Menke, W., Geophysical Data Analysis: Discrete Inverse Theory, Int. Geophys. Ser., vol. 45, 289 pp, Academic Press, San Diego, Calif., 1989.

Peterson, R.G., and T. Whitworth III, The subantarctic and polar fronts in relation to deep water masses through the southwestern Atlantic, J. Geophys. Res., 94(C8), 10,817-10,838, 1989.

Piola, A.R., and A.L. Gordon, Intermediate water in the southwest South Atlantic, Deep Sea Res., 36, 1-16, 1989.

Reid, J.L., On the total geostrophic circulation of the South Atlantic Ocean: Flow patterns, tracers, and transports, Prog. Oceanogr., 23, 149-244, 1989.

Reid, J.L., W.D. Nowlin,Jr., and W.C. Patzert, On the characteristics and circulation of the southwestern Atlantic Ocean, J. Phys. Oceanogr., 7, 62-91, 1977.

Roden, G.I., The vertical thermohaline structure in the Argentine Basin, J. Geophys. Res., 94(C1), 877-896, 1989.

Takahashi, T., J. Goddard, D.W. Chipman, and M. Noonan, Carbon chemistry in the confluence areas of the Brazil and Malvinas currents in the southwestern Atlantic Ocean: The results of the Confluence-89 expedition in September, 1989, technical report, 38 pp., Lamont-Doherty Geol. Obsery., Columbia Univ., Palisades, N.Y., 1990.

Thompson, R.O.R.Y., and R.J. Edwards, Mixing and water mass formation in the Australian Subantarctic, J. Phys. Oceanogr., 11, 1399-1406, 1981.

Tomczak, M., A multi-parameter extension of temperature/salinity diagram techniques for the analysis of nonisopycnal mixing, Progr. Oceanogr., 10, 147-171, 1981.

M. Boulahdid, ISMAL, B.P. 90 Alger 1er Novembre, Algiers, Algeria.

V.C. Garçon and K. Maamaatuaiahutapu, UMR 39, GRGS, 18, Avenue Edouard Belin, 31055 Toulouse Cedex, France.

A.P. Osiroff, Departamento de Oceanografía, Servicio de Hidrografía Naval, Avenidas Montes de Oca 2124, Buenos Aires, Argentina.

C. Provost, LODYC,Université Pierre et Marie Curie, 4, Place Jussieu, 75252 Paris Cedex, France.

(Received April 1, 1991;
revised October 1, 1991;
accepted January 28, 1992.)